THE JOURNAL OF PHYSICAL CHEMISTRY A

Article

pubs.acs.org/JPCA

Joint Experimental and Theoretical Study on Vibrational Excitation Cross Sections for Electron Collisions with Diacetylene

Roman Čurík,*[,†] Ivana Paidarová,[†] Michael Allan,[‡] and Petr Čársky*[,†]

[†]J. Heyrovský Institute of Physical Chemistry, Academy of Sciences of the Czech Republic, v.v.i., Dolejškova 3, 18223 Prague 8, Czech Republic

[‡]Department of Chemistry, University of Fribourg, Chemin du Musée 9, CH-1700 Fribourg, Switzerland

Supporting Information

ABSTRACT: We have measured and calculated differential and integral cross sections for elastic and vibrationally inelastic electron scattering by diacetylene molecules at electron energies from 0.5 to 20 eV in the whole range of scattering angles from 0 to 180°. The calculations were carried out using the discrete momentum representation method (DMR), which is based on the two-channel Lippmann−Schwinger equation in the momentum space. The interaction between the scattered electron and the target molecule is described by the exact static-exchange potential. Correlation−polarization forces are included by a local density functional theory. Energy dependences of integral and differential cross sections are presented for all nine vibrational modes. A detailed comparison of theoretical and experimental electron energy loss spectra is presented for electron energies of 1, 5.5, 10, and 20 eV. The theory assigns symmetry of resonances that could not be determined by empirical analysis alone. The theory reveals, and quantitatively describes, the switching of partial waves accompanying excitation of nontotally symmetrical vibrations. Limitations of the theory in reproducing experimental data for the narrow π^* resonance below 2 eV are mentioned.

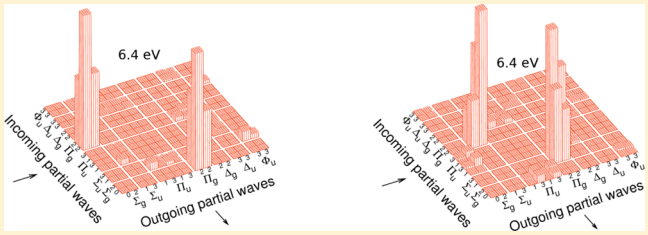

I. INTRODUCTION

This paper represents a continuation of the previous work[1,2] on diacetylene (1,3-butadiyne). The first of the two papers[1] reported on the absolute angle-differential vibrational excitation cross sections, and the other one[2] was a joint experimental and theoretical study on the absolute angle-differential elastic cross sections. As noted previously,[1,2] electron collisions with diacetylene are relevant in many practical environments, such as formation of technological plasma,[3,4] combustion,[5−7] and astronomy.[8,9] Vibrational excitation is important as a means of electron cooling and means of heating of molecules. Apart from this direct interest, vibrational excitation is also important because it is closely linked to the important electron-driven chemistry process of dissociative electron attachment—both are the result of relaxation of the nuclei on a resonant potential surface. Understanding vibrational excitation is, apart from the importance on its own, an important test of correct description of the resonant processes and thus in a certain sense a prerequisite for understanding dissociative electron attachment. We considered it therefore expedient to supplement the data published previously[1] with some new experiments and to put the tentative assignments reported previously on a firmer basis by means of scattering calculations.

II. EXPERIMENTAL SECTION

The experimental conditions of the present work were the same as in our earlier study.[2,10,11] Briefly, the measurements were performed with a spectrometer using hemispherical analyzers. Absolute values of the cross sections were determined by the relative flow technique and normalized to the calculated helium elastic cross section of Nesbet.[12] The confidence limit for the magnitudes of the inelastic cross sections is about ±25% (two standard deviations). The angular distributions were measured using the combined mechanical setting of the analyzer and magnetic deflection using a magnetic angle changer. The resolution was about 15 meV in the energy-loss mode.

III. THEORY AND COMPUTATIONAL DETAILS

Our computational method called discrete momentum representation (DMR) is a rigorous *ab initio* method based[13,14] on the two-channel Lippmann−Schwinger equation, which may be expressed as a set of two coupled matrix equations

$$\begin{pmatrix} T_{00} & T_{01} \\ T_{10} & T_{11} \end{pmatrix} = \begin{pmatrix} U_{00} & U_{01} \\ U_{10} & U_{11} \end{pmatrix} + \begin{pmatrix} U_{00} & U_{01} \\ U_{10} & U_{11} \end{pmatrix} \begin{pmatrix} G_0 & 0 \\ 0 & G_1 \end{pmatrix} \begin{pmatrix} T_{00} & T_{01} \\ T_{10} & T_{11} \end{pmatrix} \quad (1)$$

where subscripts 0 and 1, respectively, denote the elastic and a vibrationally inelastic channel for a particular vibrational mode.

Received: July 22, 2014
Revised: September 18, 2014
Published: September 18, 2014

dx.doi.org/10.1021/jp5073186 | J. Phys. Chem. A 2014, 118, 9734−9744

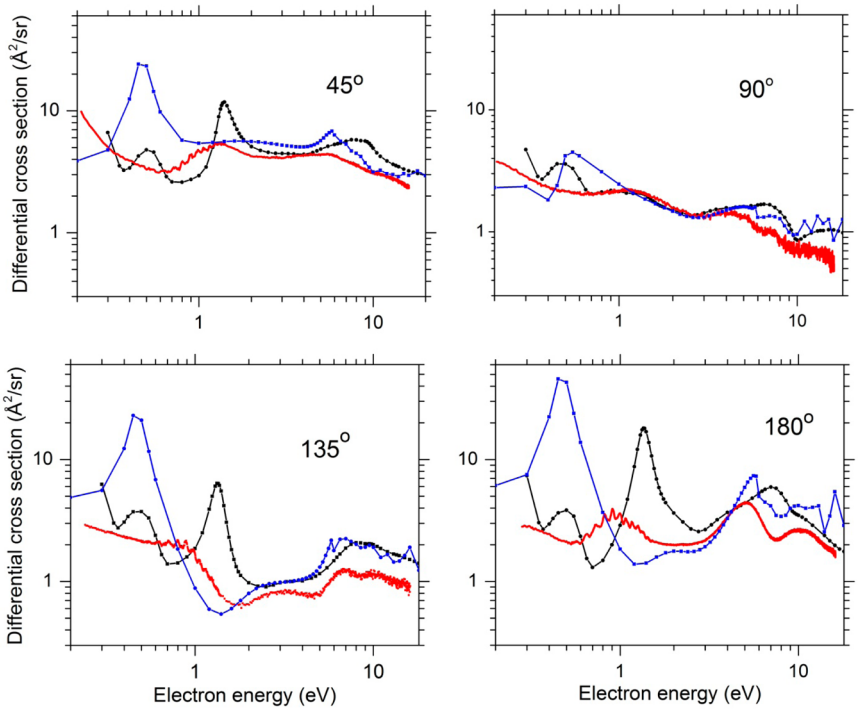

Figure 1. Energy dependence of the elastic differential cross section for four different scattering angles. Experiment[1] (red line) is compared with SMC[2] (blue line) and DMR (black line) calculations.

The matrix elements of the interaction potential U were performed at the static-exchange-plus-polarization level (SEP):

$$U = U_{SE} + U_{CP} \quad (2)$$

The static-exchange part U_{SE} of matrix elements was calculated rigorously in the *ab initio* manner, whereas the correlation−polarization part U_{CP} was modeled by a DFT-type potential corrected by a polarization asymptotic potential.[15] The matrix form of eq 1 resulted from numerical discretization of the UGT term. The details of the procedure have been described previously.[14]

The geometry of diacetylene was optimized with the valence-shell double-ζ and polarization (9s5p/4s1p)/[3s2p1d/2s1p] basis set[16] and then used for analytical evaluation of normal modes, harmonic frequencies, dipole moment and its derivatives, and density matrix and its derivatives with respect to atomic coordinates by standard quantum chemical procedures.

The long-range correction to the DFT correlation potential requires knowledge of the static polarizability tensor α_{ij} and its derivatives with respect to nuclear positions.[15] Sophisticated methods, such as the coupled cluster linear response method,[17] are computationally too expensive when used for calculation of polarizabilities and polarizability gradients of polyatomic molecules, and therefore the Kohn−Sham density functional theory (DFT) approach was used instead. Performance of DFT methods was tested[18] for a series of various exchange−correlation functionals. The molecule selected for testing was methane, and the derivatives of the polarizability tensor obtained with highly correlated wave function methods were taken as standard. This study and the unpublished test calculations on larger hydrocarbons showed that the best DFT results were obtained with the PBE0 exchange−correlation functional and Sadlej's polarized valence triple-ζ basis.[19] Dalton Release 2.0. was used for all calculations. The mean polarizability value of 47.56 au obtained for diacetylene compares reasonably well with the experimental value[20] 46.63 au and with the value of 49.10 au, obtained by the CCSD(T) calculations with a large basis set of 380 Gaussians.[21]

A direct output of scattering calculations is a manifold of calculated vibrational cross sections that can be taken as a theoretical line electron energy loss spectrum. The obtained lines were positioned at values of experimentally determined frequencies.[22,23] For a direct comparison with the measured electron energy loss spectra we assumed a Gaussian shape for each line and a half-width of 15 meV, which corresponds to the resolution of the experimental apparatus.

IV. ELASTIC SCATTERING

Elastic scattering is not of our primary interest, but we present selected elastic cross sections in this paper because good results obtained by calculations for elastic scattering are a prerequisite for meaningful predictions of cross sections for vibrationally inelastic scattering. As may be noticed in eq 1, the vibrationally inelastic channels are coupled with the elastic channel, and the accuracy achieved for the former affects strongly the accuracy obtained for the latter. Hence, to have confidence in our vibrationally inelastic results, we wanted to see how our data obtained for elastic scattering compare with the respective experimental data[1] and the results of sophisticated Schwinger multichannel (SMC) variational calculations.[2] This comparison is presented in Figure 1 for elastic differential cross section as a function of electron energy for four scattering angles. The present DMR calculations are in agreement with the SMC calculations for energies between about 2 and 16 eV. The two theoretical lines match the shape of experimental curve in this range, though both calculations overestimate experiment by up to a factor of 2.

The peak calculated at 1.33 eV by the DMR theory is due to the $^2\Pi_u$ resonance (see the symmetry assignment below). This

dx.doi.org/10.1021/jp5073186 | J. Phys. Chem. A 2014, 118, 9734−9744

resonance is manifested in the experimental spectrum as a broad band extending from about 0.6 to 1.3 eV, with vibrational (boomerang) structure. The agreement is very satisfactory in view of the fact that shape resonances are commonly calculated at slightly higher energies and that fixed-nuclei calculations yield bands narrower than experiment. A prototype case is the lowest π^* resonance in benzene at about 1.2 eV. It is hardly observable by elastic scattering experiments, but energy dependences of the integral cross section calculated by Gianturco and Luchesse[24] and Bettega and collaborators[25] exhibited strong and narrow resonances at 1.82 and 2.3 eV, respectively. Our DMR unpublished calculations for benzene gave a similar result, a sharp resonance at 1.5 eV, slightly higher than in experiment. Gianturco and Lucchese[24] proposed a plausible explanation for this discrepancy by the fact that their calculations (and also those by Bettega et al.[25]) were performed at the fixed-nuclei level that does not reproduce the Franck–Condon profile of the band and thus leads to a narrower resonance than would be obtained if coupling to nuclear motion were included. The fact that shape resonances are generally calculated at higher energies than experiment is ascribed to incomplete inclusion of polarization. We note that this shift is only about 0.3 eV in the present calculation, less than in virtually all existing calculations on polyatomic molecules, and indicative of the proper treatment of polarization in the present model.

Next we check the angular dependences. In Figure 2 we compare the DMR calculations with experimental data[2] and

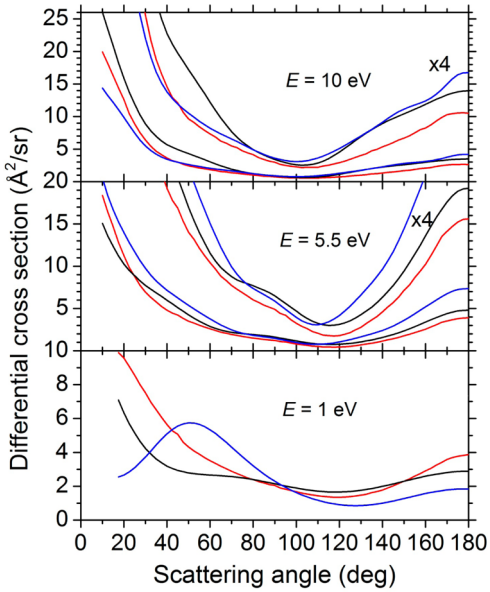

Figure 2. Angular dependence of the elastic differential cross section for electron energies of 1, 5.5, and 10 eV. Red lines are experimental results,[2] black lines are results of DMR calculations, and blue lines are results of SMC calculations.[2]

SMC calculations.[2] Results of our calculations are in agreement with experimental data and are generally slightly better than the SMC calculations. The agreement is worse for the electron energy of 1 eV and scattering angles smaller than 90°. This discrepancy is not surprising. From Figure 1 we have already learned that theoretical data for electron energies below 2 eV should be taken with caution because the calculated and experimental resonance energies are slightly different and because the Franck–Condon broadening of the resonance is not taken into account by the fixed-nuclei calculation. The excellent agreement of our calculation for electron energy of 1 eV and the scattering angle of 135° must thus be taken as partly fortuitous.

Nevertheless, we may conclude this section by stating that, although agreement with experiment is not perfect, it is good enough to reproduce the shapes of dependences of differential cross sections with respect to electron energies and scattering angles for which the experiments on vibrationally inelastic scattering were done. Hence we think that this is a good prerequisite for valuation of cross sections for vibrationally inelastic scattering.

V. VIBRATIONALLY INELASTIC SCATTERING

Electron energy dependences of vibrational data exhibit more distinct peaks than elastic data and hence provide firmer grounds for finding positions of resonances and identification of their nature. This property may be explained by a weaker background contribution to the cross section in inelastic channels. We start our exploration of resonances by Figure 3 in which we present calculated electron energy dependencies of integral cross sections for the nine normal modes of diacetylene.

We are using the energy dependence of the integral cross sections for vibrational modes as a tool for getting the first rough idea about positions of resonances. An immediate observation from Figure 3 is that the curves reveal positions of resonances by clear-cut maxima. This is in contrast to the energy dependences of elastic scattering, where observation of resonances may be obscured by a strong background nonresonant scattering. As experimental data on inelastic integral cross sections are not available, we will deal hereafter with differential cross sections only.

In Figure 4 we present the calculated energy dependence of differential cross sections for the scattering angle of 180°. This angle was chosen intentionally because the curves presented in Figure 4 are used below in our attempt to reconstruct experimental differential cross sections at two selected energy losses (shown in Figure 5). We have also calculated data for scattering angles 45° and 135°. The corresponding figures can be found in the Supporting Information. The not yet published experimental data for the scattering angle 135° has been included in the Supporting Information, too. The respective plots of differential cross sections vs electron energy are displayed there for the $\nu_{6,8}$ and ν_9 modes, and also for several overtones and combination bands.

At higher energies the vibrational energy loss spectrum of diacetylene is dominated by the C–H stretch band centered at 413 meV. It consists of the symmetric and asymmetric C–H stretch vibrations, ν_1 and ν_4, respectively. The two modes are separated by 1 meV only, and hence they are not resolved in the experiment. Absolute experimental values of the differential cross section for excitation of these two modes[1] as a function of collision energy are shown in the left panel of Figure 5. It is clear that the excitation of these stretch modes is governed by several resonances. The highest peak was assigned in ref 1 to the $^2\Pi_u$ resonance, which is followed by three bands at 4.4, 6.9, and 9.8 eV, not assigned previously.

Our calculations (black curves in Figure 5) confirm the presence of all four resonances. Computed energy positions are fairly close to the energies determined experimentally. The strongest one, the $^2\Pi_u$ resonance, was calculated at 1.33 eV,

dx.doi.org/10.1021/jp5073186 | J. Phys. Chem. A 2014, 118, 9734–9744

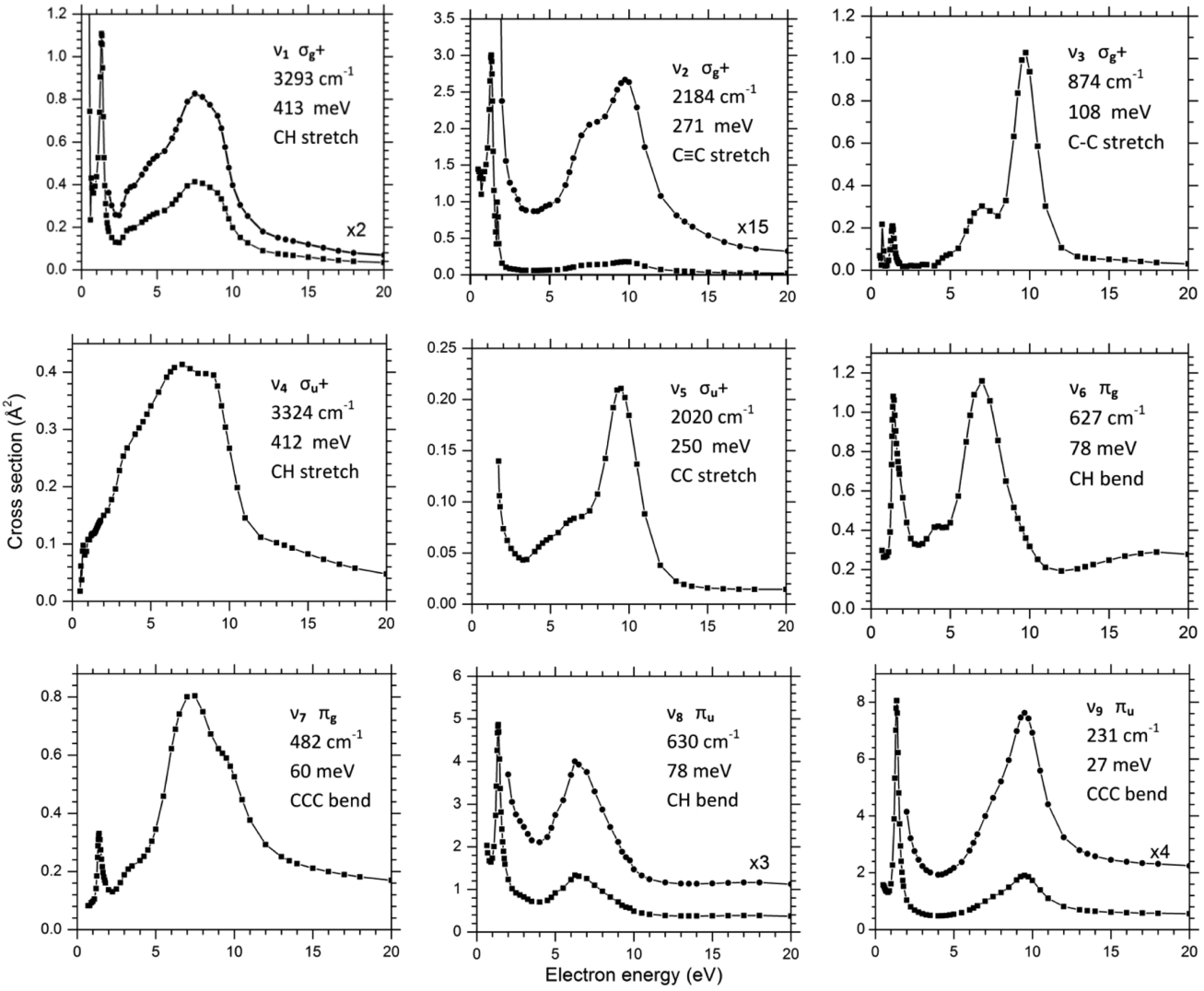

Figure 3. Calculated energy dependences of vibrationally inelastic *integral* cross sections for nine normal modes.

only slightly above the experimental value of 1.0 eV. Figure 5 indicates that this resonance is prominent in the cross section for exciting the σ_g^+ symmetric stretch mode ν_1, but nearly absent in the cross section for exciting the σ_u^+ asymmetric stretch mode ν_4, as expected on symmetry grounds. Figure 5 also shows that the calculation reproduces resonances in the 3−12 eV range, which excite both C−H stretch modes. A shoulder and four strongly overlapping peaks can be discerned in the ν_1 cross section, but a clear-cut correspondence with experiment is provided by the line for the ν_4 cross section with its three distinct peaks.

In a similar manner, we compare theoretical and experimental cross sections measured at the energy loss of 78 meV in the right panel of Figure 5. At this energy loss, a contribution to the inelastic signal comes from the excitation of the two bending modes ν_6 (π_g) and ν_8 (π_u), both having a vibrational energy of 78 meV. We estimate that the CCC bending mode ν_7 (π_g), located at 60 meV, contributes only about 3% of the signal at the energy loss at 78 meV, and we therefore did not include this mode in our analysis in Figure 5. Theory confirms the presence of the resonance seen on the experimental curve at 5.2 eV, although it is calculated about 1 eV above the experimental value. Figures 4 and 5 reveal that this resonance excites both bending modes. Theory and experiment also agree about the very broad band in the 10−20 eV range. A discrepancy in this comparison is the strong $^2\Pi_u$ resonance peak calculated at 1 eV in the ν_8 cross section, which is not as high (but broadened by Franck−Condon width) in the experimental data. We assume that the overestimated presence of the 1 eV $^2\Pi_u$ resonance in the calculated excitation of the ν_8 π_u mode can be explained by a "leak" from our elastic channel data where this resonance also appears stronger than in the experiment (Figure 1). Another difference concerns the weak narrow resonance calculated at 3 eV in the excitation of the ν_8 mode, absent in the experiment.

In this paragraph we examine angular dependences of inelastic cross sections at the energy of the 1 eV $^2\Pi_u$ resonance. In Figure 6 we present the angular dependence of the differential cross section for the vibrational mode ν_2. The observed dependence is compared with theoretical curves calculated for several electron energies in the 1 eV region. The purpose of this figure is to show that the excitation of the ν_2 mode is strongly dependent on both the electron energy and the scattering angle. It is evident that a resonance-dominated cross section cannot be well reproduced unless both the calculation and the experiment are performed at the center of the resonance, which is slightly higher in the theory (Figures 3−5). This is confirmed in Figure 6 where the best agreement

dx.doi.org/10.1021/jp5073186 | J. Phys. Chem. A 2014, 118, 9734−9744

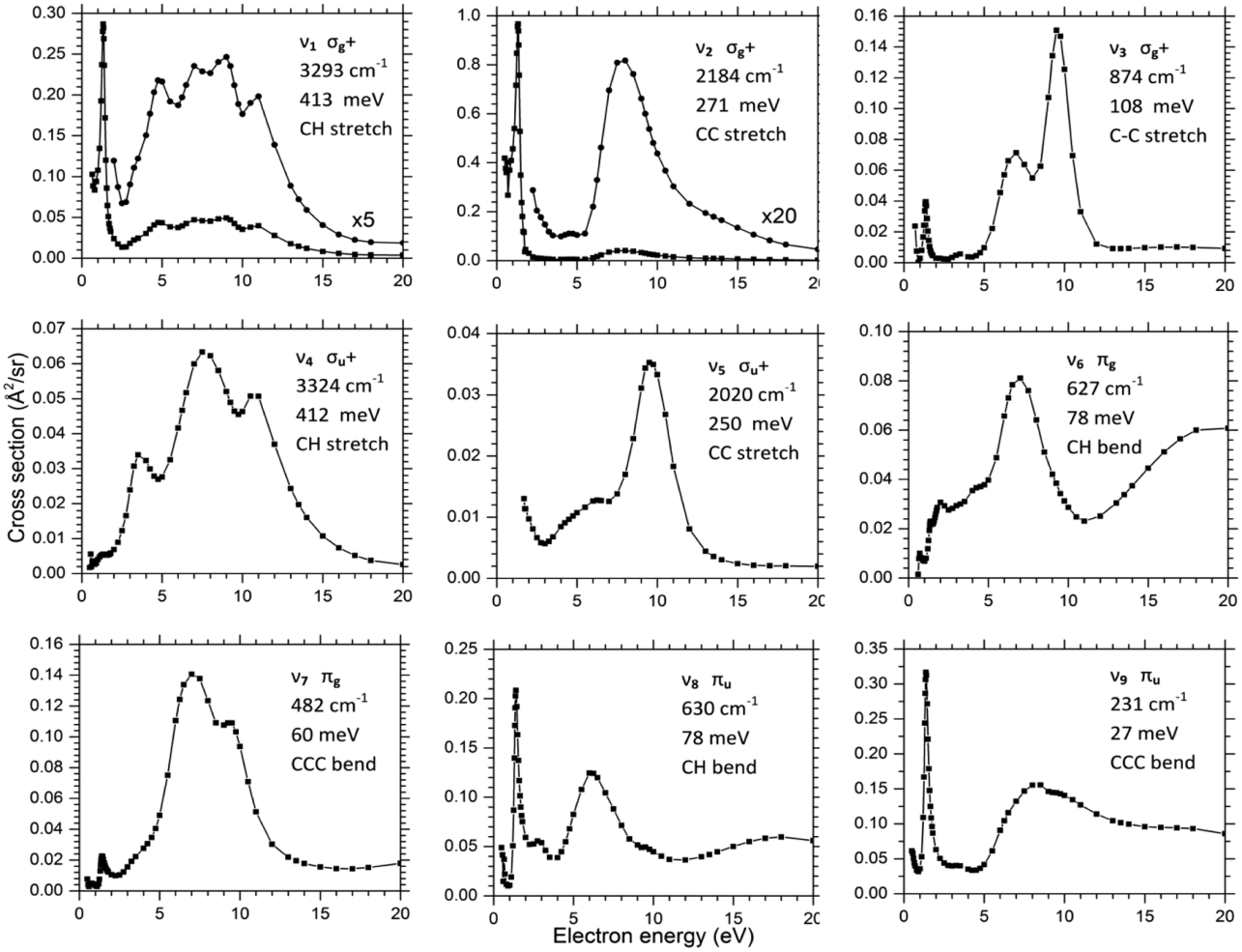

Figure 4. Calculated energy dependences of vibrationally inelastic *differential* cross sections for nine normal modes at 180°.

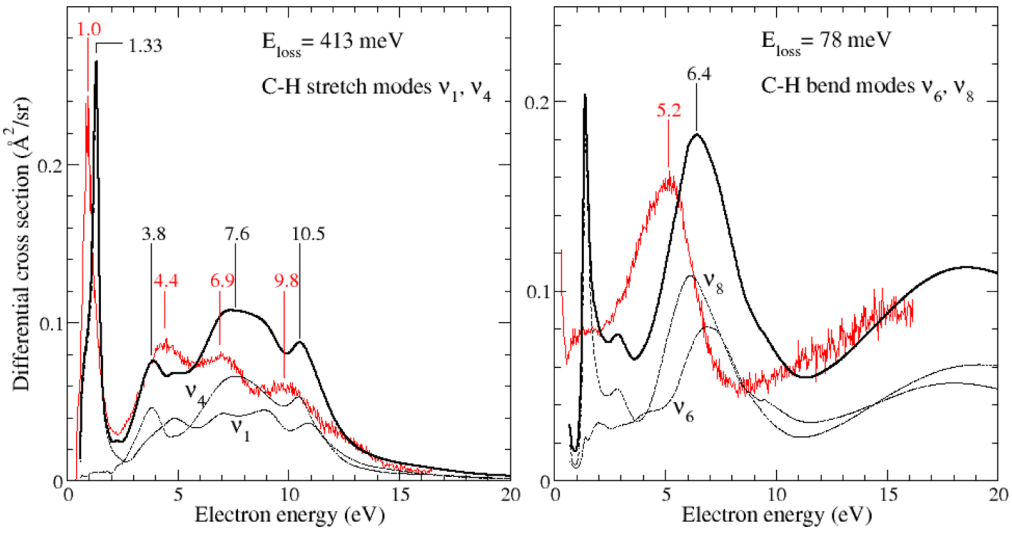

Figure 5. Computed (black curves) and measured (red lines) data for vibrationally inelastic differential cross section at the two energy losses indicated. The scattering angle is 180°. Both curves are in absolute scale, no scaling was performed. Dashed lines show contributions from the individual vibrational modes.

is obtained for calculation at the energy of 1.33 eV, the calculated position of the resonance. This problem that arises when theory is compared to experiment at, or close to, energies of sharp resonances, has been known for a long time. A detailed discussion with sound physical arguments can be found in the paper by Sun et al.[26]

Angular distributions for the C−H bending modes ν_6 and ν_8 are displayed in Figure 7. As mentioned above, they cannot be

dx.doi.org/10.1021/jp5073186 | J. Phys. Chem. A 2014, 118, 9734−9744

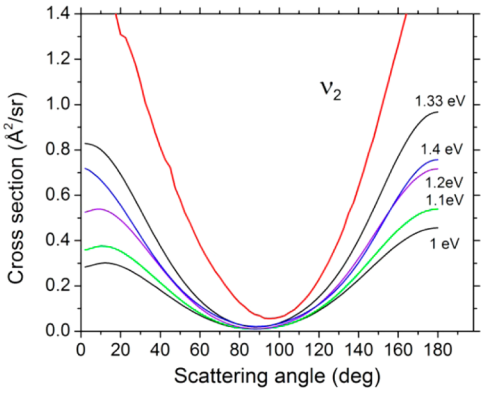

Figure 6. Angular dependence of the differential cross section for the vibrational mode ν_2. The red line is the experimental result recorded at 1 eV, the center of the $^2\Pi_u$ resonance; the other lines are results of DMR calculations obtained for different electron energies.

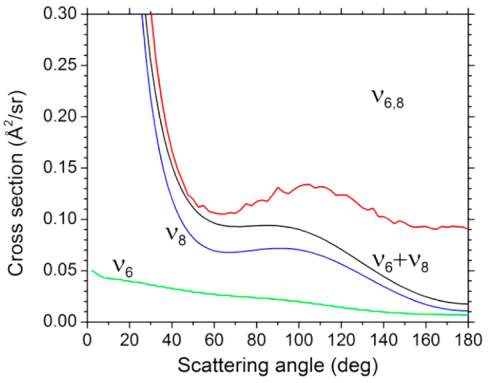

Figure 7. Angular dependence of the sum of differential cross sections for vibrational modes $\nu_{6,8}$ and for electron energy 1 eV. The red line is experiment, the black line is the $\nu_{6,8}$ result of DMR calculations, and the green and blue lines are calculated results for individual ν_6 and ν_8 modes, respectively.

resolved experimentally and we therefore compare the experimental data with the sum of the theoretical cross sections in Figure 7. We neglect a small contribution from the ν_7 mode. Our computed $\nu_6 + \nu_8$ differential cross section underestimates the experimental signal for larger scattering angles, whereas the agreement is very good for scattering angles under 60°. The difference can again be explained by the chosen collision energy of 1 eV, which is the experimental position of the $^2\Pi_u$ resonance but it is shifted from the computed resonance position by 330 meV. Here the scattering at small scattering angles is dominated by the infrared activity of the ν_8 mode whereas the large scattering angles are strongly influenced by the resonance mechanism.

In Figures 8 and 9 we attempt to reconstruct computationally the electron energy loss spectra for electron energies of 1, 5.5, 10, and 20 eV. As already noted in the section on elastic scattering, and documented by Figure 1, the energy region below 2 eV is difficult for the theory to treat. First, the $^2\Pi_u$ resonance is calculated at 1.33 eV instead of 1.0 eV as observed experimentally, and second, the fixed-nuclei approximation cannot reproduce the Franck−Condon profile of the band, making it too narrow and high. Hence, the results of the theory in Figure 8 for the electron energy of 1 eV should be taken with caution. With these limitations in mind, it is seen in Figure 8 that for 1 eV the DMR theory is close to experiment in terms of the relative intensities of the different modes, but about by a factor of 3 too low.

The energy-loss regions between 130 and 200 and from 300 to 400 meV are due to overtones and combination bands and cannot be supported by the present calculations based on harmonic approximation. The predictive power is limited, therefore, to 1 ← 0 vibrational transitions only. This limitation is more important in the present case, where the electron energy loss spectra are rich in overtones and combination bands, than in molecules with exclusively broad resonances like methane,[27] The spectra at the 1 eV electron energy were also measured at the scattering angles 0, 20, 45, 90, and 180°, and the respective plots are contained in the Supporting Information. The experimental electron energy loss spectrum for 5.5 eV has a rich region of overtones and combination bands between 450 and 1000 meV and we considered it expedient to show it in Figure 8, even though it cannot be

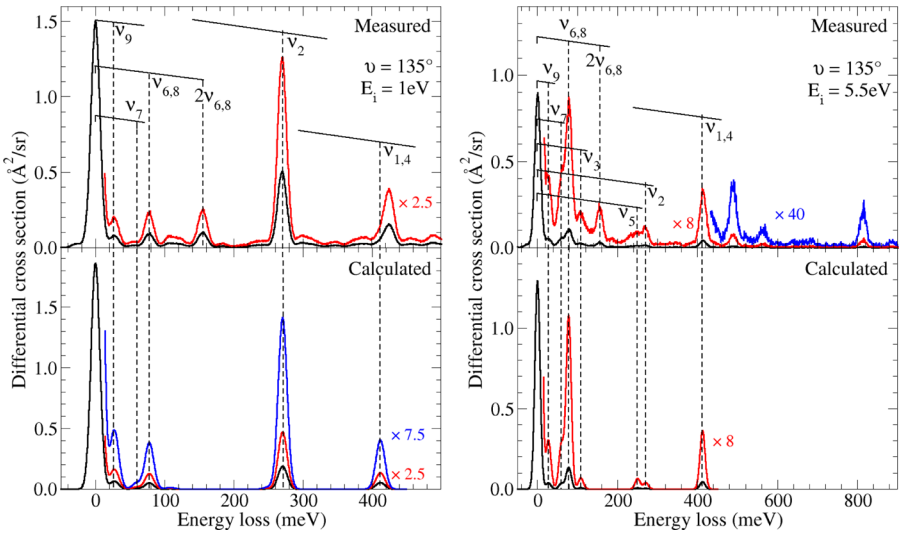

Figure 8. Electron energy loss spectra for collision energies of 1 eV (left panel) and 5.5 eV (right panel). Upper panels show present experimental data, and lower panels display calculated spectra.

dx.doi.org/10.1021/jp5073186 | J. Phys. Chem. A 2014, 118, 9734−9744

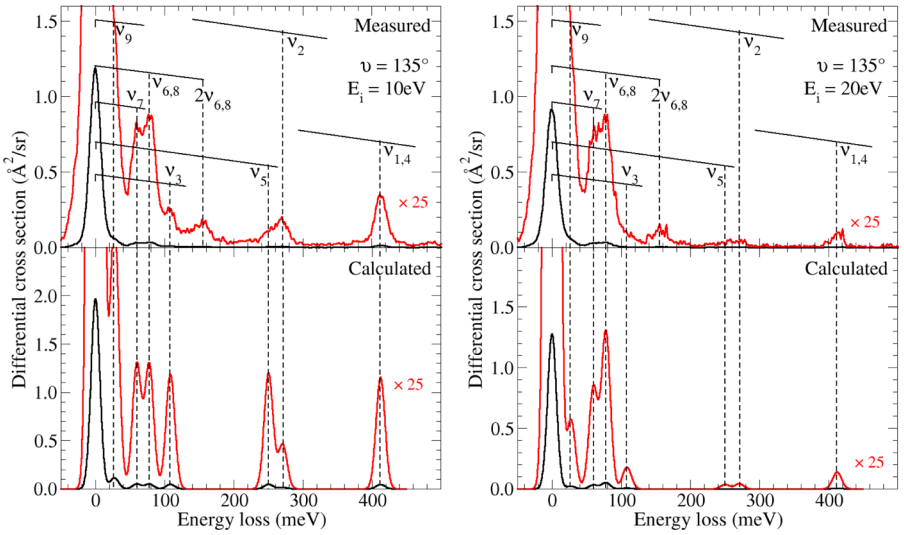

Figure 9. Electron energy loss spectra for collision energies of 10 eV (left panel) and 20 eV (right panel). Upper panels show present experimental data, and lower panels display calculated spectra.

interpreted by our calculations because of the use of harmonic approximation.

In contrast to the 1 eV case, at 5.5 eV the agreement between experiment and theory for the region of normal modes is very good even in terms of absolute values, except perhaps that the differential cross sections for the weak ν_2 and ν_5 modes are calculated slightly too low. Again, the observed signal between 130 and 200 meV, assigned tentatively to $2\nu_{6,8}$, cannot be supported by our calculations because the theoretical model is based on a harmonic approximation. Interpretation of spectra recorded at the electron energy of 10 eV is complicated by the circumstance that the DMR theory predicts a strong resonance at 9.5 eV, which was not observed in any experiment done so far. The differential cross section for the elastic peak is overestimated by about a factor of 2, in accordance with Figure 1. Intensities of vibrational bands relative to the elastic peak are well reproduced for the ν_2, $\nu_{6,8}$, and ν_7 modes but overestimated for the ν_3 and ν_5, and to a lesser extent also for both components of the $\nu_{1,4}$ peak. This discrepancy is in accordance with Figure 5 showing a strong resonance at 9.5 eV (not observed in experiments) for ν_3 and ν_5 modes and to a lesser extent also for ν_1 and ν_4 modes. In the 20 eV energy region, where there are no resonances, agreement between experiment and theory is excellent. Not only are the relative differential cross sections correctly reproduced, but also theoretical and experimental data are close in absolute value. The strongest peak at 78 meV is due to the overlap of CH bending modes ν_6 π_g and ν_8 π_u. According to our calculations the respective differential cross section are 0.025 and 0.027 Å^2/sr. As with the other electron energies assumed in this paper, the observed signal between 130 and 200 meV, assigned tentatively to $2\nu_{6,8}$, cannot be reproduced by our calculations because of the harmonic approximation.

VI. ASSIGNMENT OF SYMMETRIES TO RESONANCES

In this section we show that explicit inclusion of the vibrationally inelastic channel into the theoretical model is profitable for examination of energy positions and symmetries of shape resonances. The background cross section is low and it enables us to see the positions of resonances more distinctly than is possible with elastic scattering. On the other hand, allowing for vibrational motion makes the assignment more complex. We will show that more than one resonance and more than one symmetry component may be involved in the resonant vibrational excitation of polyatomic molecules. We will be dealing with one-electron (shape) resonances only, and hence, for simplicity, we drop the doublet symbol attached to the symmetry component, e.g., $^2\Pi_u$ will be denoted hereafter as Π_u.

Our aim is to analyze the resonances shown in Figure 5 and also to determine the dominant symmetry components that drive the resonant processes. The left panel of Figure 5 suggests that there are at least four resonances connected with the vibrational modes ν_1 and ν_4. On the calculated curve for ν_4 we see them at energies 3.8, 7.6, and 10.5 eV; on the calculated curve for ν_1 there are even more, but less pronounced, resonances. The overall shape of the calculated sum (ν_1 and ν_4) curve is in good agreement with the experiment. The respective differences in calculated and observed resonance energy positions do not exceed 0.7 eV. In the right panel of Figure 5 we will analyze the resonance enhancing the calculated excitation of ν_6 and ν_8 modes around 6.4 eV. Experimentally, the resonance is observed at 5.2 eV.

The tool for examination of symmetries of the resonances exploits the data provided by the DMR method. In particular, the tool is based on postprocessing the matrix elements of the inelastic T-matrix block $\mathbf{T_{10}}$, obtained by solving the Lippmann−Schwinger equation (eq 1). Although the elements are evaluated on a numerical angular grid (specified by Lebedev quadrature), their transformation to partial-wave representation $T_{lm,l'm'}$ is straightforward. Then the partial waves, specified by the pair (lm), may be combined in such a way that they belong to irreducible representations of the point group $D_{\infty h}$. In the present analysis of the resonance symmetries we have limited our angular space by $l \leq 3$; i.e., we included the lowest 16 partial waves. They can be combined into 7 irreducible representations Γ ordered as follows: Σ_g, Σ_u, Π_u, Π_g, Δ_g, Δ_u, Φ_u. The transformation may be written as

$$T_{ij}^{\Gamma} = \sum_{lm,l'm'} b_{i,lm}^{\Gamma} T_{lm,l'm'} b_{j,l'm'}^{\Gamma} \qquad (3)$$

dx.doi.org/10.1021/jp5073186 | J. Phys. Chem. A 2014, 118, 9734−9744

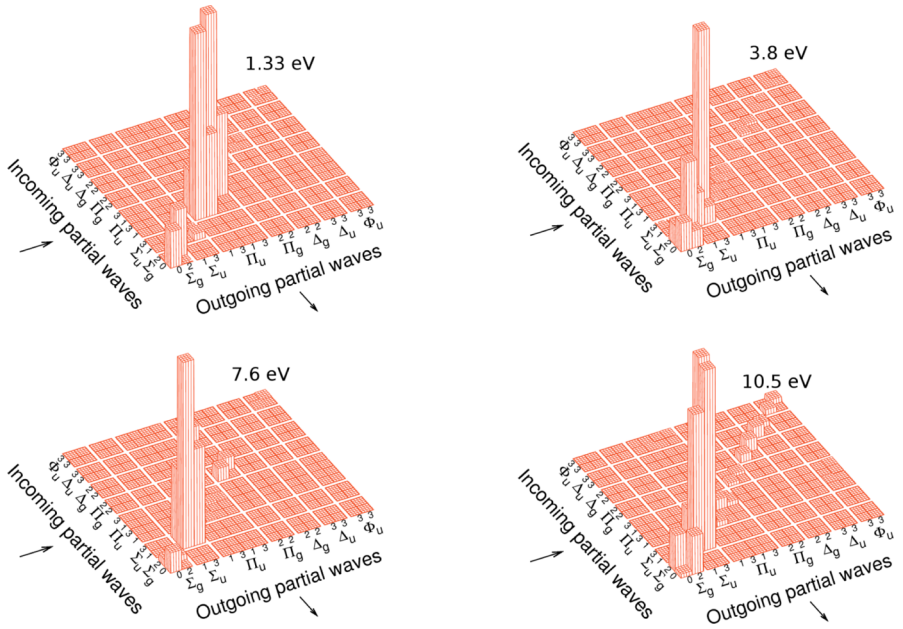

Figure 10. Symmetric C−H stretch mode ν_1. Heights of the vertical bars are the values of inelastic squared elements $|T^{\Gamma}_{i,j}|^2$ calculated from eq 3. The integer numbers closest to the graph represent the angular quantum number l of each angular function belonging to the symmetry component.

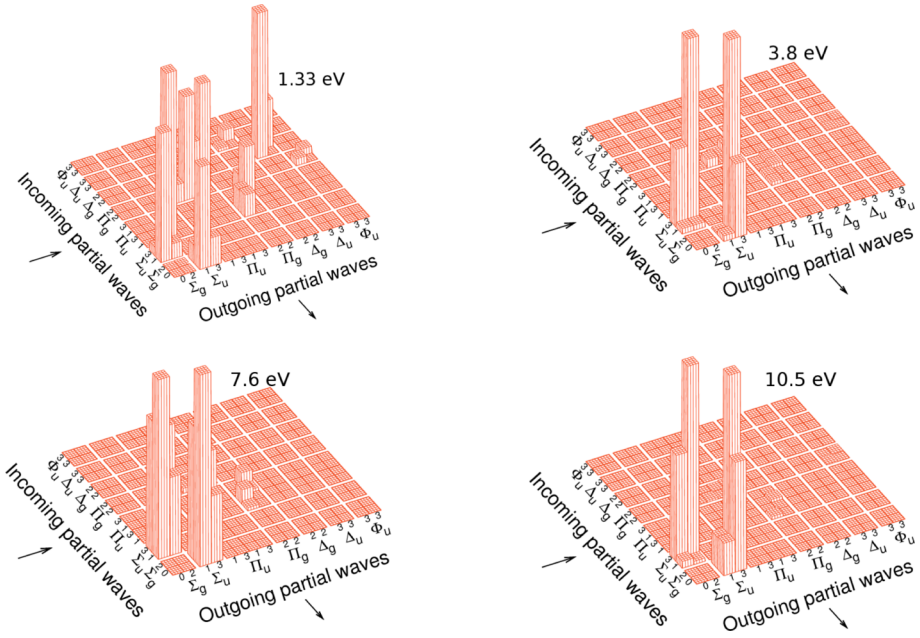

Figure 11. Antisymmetric C−H stretch mode ν_4. Details are explained in caption of Figure 10.

where the coefficients $b^{\Gamma}_{i,lm}$ form a unitary matrix and can be found in the literature for most of the point groups.[28] Sum of the squared elements $|T^{\Gamma}_{i,j}|^2$ (with all the partial waves included) forms the inelastic integral cross section. The individual squared elements $|T^{\Gamma}_{i,j}|^2$ in the limited angular space $l \leq 3$ are displayed in Figure 10 as vertical bars for the symmetric C−H stretch mode ν_1. We displayed them for four energies, for which we observe resonant behavior in excitation of the mode ν_1 (Figure 5). Figure 10 demonstrates that only very few partial waves have a non-negligible contribution to the inelastic cross section at the resonant energies.

The top left panel of Figure 10 clearly shows that at the 1.33 eV resonance, the dominant contribution to the computed cross section, comes from the Π_u symmetry with a weak contribution from the Σ_g component. The Π_u symmetry was already assigned previously.[1,2] Thus, the top left panel of Figure 10 gives more detailed information, according to which the incoming flux of the scattered electron is divided into the dominant Π_u symmetry component and a less important Σ_g component. After the excitation of symmetric ν_1 mode, the electron leaves the molecule keeping its symmetry components.

Mechanism of resonant excitation for the band at 3.8 eV in Figure 5 is similar, but here the dominant contribution comes from the Σ_u symmetry with a weak contribution of the Σ_g component. The resonant mechanism at 7.6 eV is also driven by the Σ_u symmetry; however, there is a weak presence of the Σ_g and Π_g components as well. Finally, at the last resonant energy of 10.5 eV (bottom right panel of Figure 10), the

dx.doi.org/10.1021/jp5073186 | J. Phys. Chem. A 2014, 118, 9734−9744

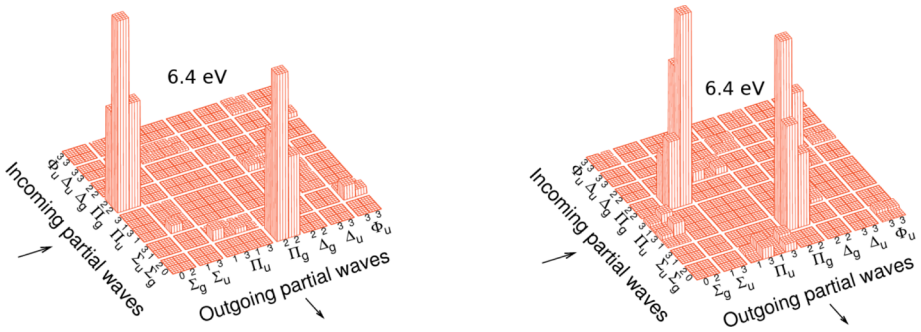

Figure 12. C−H bend modes ν_6 (left panel) and ν_8 (right panel). Details are explained in caption of Figure 10.

Table 1. Comparison of Calculated and Experimental Resonance Positions Together with the Symmetries Relevant for the Resonant Vibrational Excitation Process

experimental resonant energies (eV)	1.0	4.4	6.9	9.8	5.2
theoretical resonant energies (eV)	1.33	3.8	7.6	10.5	6.4
symmetry for ν_1	Π_u	Σ_u	Σ_u	Σ_u	
symmetry for ν_4		$\Sigma_u \leftrightarrow \Sigma_g$	$\Sigma_u \leftrightarrow \Sigma_g$	$\Sigma_u \leftrightarrow \Sigma_g$	
symmetry for ν_6					$\Pi_g \leftrightarrow \Sigma_g$
symmetry for ν_8					$\Pi_g \leftrightarrow \Sigma_u$

vibrational excitation of the ν_1 mode is again driven mainly by the Σ_u symmetry resonance with a weak Σ_g contribution. The visible contribution of higher symmetries reflects a simple fact that the resonant process at 10.5 eV is less pure and the inelastic cross section contains also a non-negligible background. We conclude the symmetry analysis of resonances for ν_1 mode by a note that all the symmetries involved in these resonant processes are in accord with the resonance symmetry selection rules of Wong and Schulz.[29]

The second vibrational mode that contributes to the inelastic cross section shown in the left panel of Figure 5 is the antisymmetric C−H stretch mode ν_4. Results of the analysis for this mode are shown in Figure 11, similarly as was done for the ν_1 in Figure 10. When comparing it to Figure 10, we observe two major differences:

1. The cross section at 1.33 eV (top left panel of Figure 11) is scattered into many partial wave contributions and this feature suggests there is no resonant mechanism available. This observation is in agreement with the shape of the Π_u orbital.[1] Accordingly, Figure 4 does not show any peak at 1.33 eV in the ν_4 cross section.
2. The mechanisms at 3.8, 7.6, and 10.5 eV are clearly resonant, but in contrast to excitation of ν_1 mode, they are not diagonal and they couple Σ_g and Σ_u symmetry components. At these energies, Figure 11 describes a resonant process in which the scattered electron enters the molecular system in the Σ_g symmetry, excites the antisymmetric C−H stretch mode ν_4, and then leaves the molecule in the Σ_u symmetry component. The fact that there are two groups of columns, arranged symmetrically across the diagonal, is due to the principle of microscopic reversibility; i.e., the symmetries of the incoming and outgoing waves can be switched. All the three resonances are exempts from the symmetry selection rules of Wong and Schulz.[29]

Figure 12 displays a symmetry analysis of a single resonance that dominates the cross section for excitation of the C−H bending modes ν_6 and ν_8, shown on the right panel of Figure 5. The results demonstrate that the excitation of C−H bending modes requires coupling between the Σ and Π symmetries. The scattering calculations show (Figure 12) that the Π_g resonance drives the excitation of both modes; however, in the case of the π_g mode ν_6 it couples with the Σ_g resonance, whereas in the case of the π_u mode ν_8 it couples with the Σ_u resonance. A summary of the above analysis for all the four modes ν_1, ν_4, ν_6, and ν_8 is displayed in Table 1.

Hence, the calculations predict that the resonant excitation of the ν_1 and ν_4 C−H stretch modes is rather complex. The partial wave analysis reveals Σ_u incoming ↔ Σ_u outgoing waves for ν_1 (σ_g) excitation and Σ_g incoming ↔ Σ_u outgoing waves for ν_4 (σ_u) excitation, at three energies (3.8, 7.6, and 10.5 eV) within the 3−12 eV range. The presence of several relatively narrow σ^* resonances at the relatively high energies is unusual and in contrast to what is found, for example, in saturated hydrocarbons, where only one extremely broad band is observed in the C−H stretch excitation. We ascribe it to the relatively high symmetry of diacetylene, which prevents the electron from leaking out as s-wave in the elastic channel for the Σ_u resonances. Recall that the present model does not permit calculation of core-excited resonances.

Interesting insight has also been gained into the excitation via the "second π^*" resonance $^2\Pi_g$, originally observed as a band at 6.2 eV in the ν_2 C≡C stretch excitation.[1] The present calculation places it at 6.4 eV, in good agreement with the experiment, and shows that it is, unexpectedly, also very efficient in the excitation of the non-totally symmetrical C−H bend vibrations ν_6 (π_g) and ν_8 (π_u), but that in this case the vibrational excitation couples the incoming Π_g wave with an outgoing Σ_g (for ν_6) or Σ_u (for ν_8) waves (or going from Σ_g or Σ_u to Π_g, because of the microscopic reversibility). The experimental band in the ν_6/ν_8 excitation cross section is at a lower energy (at 5.2 eV) and we propose that dependence of the peak position on the final channel, quite common in electron scattering, is due to Franck−Condon effects. The (real part of) the potential hypersurface of the $^2\Pi_g$ anion state has a complex shape. It goes up along the ν_2 normal coordinate but goes down along the ν_6 and ν_8 normal coordinates (simple electronic structure calculation reveals that the C−H bonds are bent in the diacetylene anion). This is likely to cause the cross

dx.doi.org/10.1021/jp5073186 | J. Phys. Chem. A 2014, 118, 9734−9744

sections to peak at different energies for the same resonance but different final normal modes.

VII. SUMMARY

This paper presents a thorough theoretical analysis of elastic and, primarily, vibrationally inelastic electron scattering by diacetylene. The results are compared to experimental cross sections, in part published previously,[1] in part presented here for the first time. The calculations support and extend previous tentative assignments[1] and provide detailed information on the observed resonances. The strengths of the present calculations are an advanced determination of the target polarization resulting in good accuracy of calculated resonance energies, absolute cross section values, and partial wave analysis which calculates which incoming and outgoing partial waves are responsible for the excitation of a given vibrational mode at a given energy, thus providing a detailed insight into the excitation mechanism.

The lowest resonance is calculated at 1.33 eV, only slightly above the experimental value of 1.0 eV. The partial wave analysis confirms the assignment as the $^2\Pi_u$ resonance, with a temporary occupation of the lowest virtual orbital π_u. This low-lying $^2\Pi_u$ resonance makes the diacetylene molecule a difficult case for a theoretical treatment, because, presumably, for its quantitative treatment it is necessary to go beyond the fixed-nuclei approximation.

The overall calculated profile in the 3−12 eV range is in good agreement with experiment although the band overlap prevents observation of all the calculated bands individually. The partial wave analysis reveals resonances for ν_1 (σ_g) excitation and ν_4 (σ_u) excitation, at three energies (3.8, 7.6, and 10.5 eV), and the "second π^*" resonance $^2\Pi_g$, originally observed as a band at 6.2 eV in the ν_2 C≡C stretch excitation.[1] According to the present calculations it is coupled with the symmetrical C−H bend vibrations ν_6 (π_g) and ν_8 (π_u). On the basis of our calculations, we thus suggest that the present commonly accepted understanding of resonant vibrational excitation of polyatomic molecules[29] should be extended. We observe that in the case of the ν_4, ν_6, and ν_8 modes, the symmetry of the resonant wave function changes during the collision. Such a mechanism allows for resonant vibrational excitation of these modes.

Although the diacetylene molecule is a difficult case for a theoretical treatment, the DMR calculations provided a good account for all scattering phenomena observed in this study for normal modes. They are beneficial in providing additional information not amenable to experiment, in particular for normal modes close in energy that cannot be distinguished because of a limited resolution of the experimental setup. A major asset is the capacity of the present theory to qualitatively calculate excitations with symmetry change and its ability to determine symmetry of resonances on sound theoretical grounds.

■ ASSOCIATED CONTENT

Supporting Information

Additional information obtained from calculations is provided by Figures S1 and S2 in which energy dependences of vibrationally inelastic cross sections for 45 and 135° are plotted in the same manner as in Figure 4 for 180°. Additional experimental results are provided by Figures S3−S5 with the overview of energy-loss spectra at the incident electron energy of 1 eV at six different scattering angles (S3), energy dependences of cross sections recorded at 135° for energy losses at 0, 27, 78, and 155 meV (S4), and also higher-lying vibrational states (S5). This material is available free of charge via the Internet at http://pubs.acs.org.

■ AUTHOR INFORMATION

Corresponding Authors

*Roman Čurík. E-mail: roman.curik@jh-inst.cas.cz.
*Petr Čársky. E-mail: carsky@jh-inst.cas.cz.

Author Contributions

The manuscript was written through contributions of all authors. All authors have given approval to the final version of the manuscript

Notes

The authors declare no competing financial interest.

■ ACKNOWLEDGMENTS

We are glad having this opportunity to pay homage to our esteemed friend Franco Gianturco for his outstanding contribution to the development of theoretical models for electron scattering by polyatomic molecules, in which we found great inspiration for our own work. We acknowledge the funding by the Grant Agency of the Czech Republic (grant P208/11/0452). This work was conducted within the framework of the COST Action CM1301 (CELINA), supported also by the Czech Ministry of Education (Grant LD14088) and by the Swiss National Science Foundation (project No. 200020-144367).

■ ADDITIONAL NOTE

This paper was originally submitted for the "Franco Gianturco Festschrift", published as the August 21, 2014, issue of *J. Phys. Chem. A* (Vol. 118, No. 33).

■ REFERENCES

(1) Allan, M.; May, O.; Fedor, J.; Ibănescu, B. C.; Andric, L. Absolute Angle-Differential Vibrational Excitation Cross Sections for Electron Collisions with Diacetylene. *Phys. Rev. A* **2011**, *83*, 052701−1−9.

(2) Allan, M.; Winstead, C.; McKoy, V. Absolute Single-Differential Elastic Cross Sections for Electron Collisions with Diacetylene. *Phys. Rev. A* **2011**, *83*, 062703−1−5.

(3) Benedikt, J.; Consoli, A.; Schulze, M.; von Kendell, A. Time-Resolved Molecular Beam Mass Spectrometry of the Initial Stage of Particle Formation in an Ar/He/C_2H_2 Plasma. *J. Phys. Chem. A* **2007**, *111*, 10453−10459.

(4) Mao, M.; Benedikt, J.; Consoli, A.; Bogaerts, A. New Pathways for Nanoparticle Formation in Acetylene Dusty Plasmas: A Modelling Investigation and Comparison with Experiments. *J. Phys. D Appl. Phys.* **2008**, *41*, 225201−1−14.

(5) Gu, X.; Guo, Y.; Mebel, A. M.; Kaiser, R. I. Chemical Dynamics of the Formation of 1,3-Butadiynyl Radical ($C_4H(X^2\Sigma^+)$) and Its Isotopomers. *J. Phys. Chem. A* **2006**, *110*, 11265−11278.

(6) Gueniche, H. A.; Glaude, P. A.; Fournet, R.; Battin-Leclerc, F. Rich Premixed Laminar Methane Flames Doped by Light Unsaturated Hydrocarbons. *Combust. Flame* **2007**, *151*, 245−261.

(7) D'Anna, A.; Alle, M.; Apicella, B.; Tregrossi, A.; Ciajolo, A. Effect of Fuel/Air Ratio and Aromaticity on Sooting Behavior of Premixed Heptane Flames. *Energy Fuels* **2007**, *21*, 2655−2662.

(8) Shemansky, D. E.; Stewart, A. I. F.; West, R. A.; Esposito, L. W.; Hallen, J. T.; Liu, X. The Cassini UVIS Stellar Probe of the Titan Atmosphere. *Science* **2005**, *308*, 978−982.

(9) Burgdorf, M.; Orion, G.; van Cleve, J.; Meadows, V.; Houck, J. Detection of New Hydrocarbons in Uranus' Atmosphere by Infrared Spectroscopy. *Icarus* **2006**, *184*, 634−637.

(10) Allan, M. Absolute Angle-Differential Elastic and Vibrational Excitation Cross Sections for Electron Collisions with Tetrahydrofuran. *J. Phys. B At. Mol. Opt. Phys.* **2007**, *40*, 3531−3544.
(11) Allan, M. Electron Collisions with CO: Elastic and Vibrational Excitation Cross Sections. *Phys. Rev. A* **2010**, *81*, 042706−1−9.
(12) Nesbet, R. K. Variational Calculations of Accurate e^--He Cross Sections below 19 eV. *Phys. Rev. A* **1979**, *20*, 58−70.
(13) Čársky, P.; Čurík, R. Vibrational Spectra by Electron Impact: Theoretical Model for Intensities. In *Computational Chemistry: Reviews of Current Trends*; Leszcsynski, J., Ed.; World Scientific: Singapore, 2006; Vol. *10*, pp 121−137.
(14) Čársky, P.; Čurík, R. Vibrational Excitation of Polyatomic Molecules. In *Low-Energy Electron Scattering by Molecules, Biomolecules and Surfaces*; Čársky, P., Čurík, R., Eds.; CRC Press, Taylor & Francis Group: Boca Raton, FL, 2012; pp 263−282.
(15) Čurík, R.; Šulc, M. Towards Efficient *Ab Initio* Calculations of Electron Scattering by Polyatomic Molecules: III. Modelling Correlation-Polarization Interactions. *J. Phys. B At. Mol. Opt. Phys.* **2010**, *43*, 175205−1−8.
(16) Dunning, T. H., Jr.; Hay, P. J. Gaussian Basis Sets for Molecular Calculations. In *Modern Theoretical Chemistry*; Schaefer, H. F., III, Ed.; Plenum Press: New York, 1977, Vol. *3*, pp 1−27.
(17) Paidarová, I.; Čurik, R.; Sauer, S. P. A. Calculations of Polarizabilities and Their Gradients for Electron Energy Loss Spectroscopy. *Collect. Czech. Chem. Commun.* **2008**, *73*, 1509−1524.
(18) Paidarová, I.; Sauer, S. P. A. *International Conference of Computational Methods in Sciences and Engineering 2009 (ICCMSE 2009)*; Simos, T. E., Maroulis, G., Eds.; Book Series: AIP Conference Proceedings; AIP: Melville, NY, 2012, No. 1504, p 695.
(19) Sadlej, A. J. Medium-Size Polararized Basis Sets for High-Level Correlated Calculations of Molecular Electric Properties. *Collect. Czech. Chem. Commun.* **1988**, *53*, 1995−2016.
(20) Gussoni, M.; Rui, M.; Zerbi, G. Electronic and Relaxation Contribution to Linear Molecular Polarizability. An Analysis of the Experimental Values. *J. Mol. Struct.* **1998**, *447*, 163−215.
(21) Karamanis, P.; Maroulis, G. Single (C-C) and Triple (C≡C) Bond-Length Dependence of the Static Electric Polarizability and Hyperpolarizability of H-C≡C-C≡C-H. *Chem. Phys. Lett.* **2003**, *376*, 403−410.
(22) Shimanuchi, T. *Tables of Molecular Vibrational Frequencies Consolidated*; National Bureau of Standards: Gaithersburg, MD, 1972; Vol. *1*.
(23) Freud, I.; Halford, R. S. Motions of Molecules in Condensed Systems. XIII. Polarized Infrared Spectrum of Single Crystals of Diacetylene. *J. Chem.. Phys.* **1965**, *42*, 4131−4137.
(24) Gianturco, F. A.; Lucchese, R. R. One-Electron Resonances and Computed Cross Sections in Electron Scattering from the Benzene Molecule. *J. Chem. Phys.* **1998**, *108*, 6144−6159.
(25) Bettega, M. H. F.; Winstead, C.; McKoy, V. Elastic Scattering of Low-Energy Electrons by Benzene. *J. Chem. Phys.* **2000**, *112*, 8806−8812.
(26) Sun, W.; Morrison, M. A.; Isaacs, W. A.; Trail, W. K.; Alle, D. T.; Gulley, R. J.; Brennan, M. J.; Buckman, S. J. Detailed Theoretical and Experimental Analysis of Low-Energy-N_2 Scattering. *Phys. Rev. A* **1995**, *52*, 1229−1256.
(27) Čurík, R.; Čársky, P.; Allan, M. Vibrational Excitation of Methane by Slow Electrons Revisited: Theoretical and Experimental Study. *J. Phys. B At. Mol. Opt. Phys.* **2008**, *41*, 115203−1−7.
(28) Altmann, S. L.; Bradley, C. J. On the Symmetries of Spherical Harmonics. *Philos. Trans. R. Soc. London A* **1963**, *255*, 199−215.
(29) Wong, S. F.; Schulz, G. J. Vibrational Excitation in Benzene by Electron Impact via Resonances: Selection Rules. *Phys. Rev. Lett.* **1975**, *35*, 1429−1432.
(30) Gallup, G. A. Symmetry Selection Rules for Vibrational Excitation by Resonant Electron Impact and a Unified Treatment of Vibronic Coupling between Resonances and to the Continuum: A Complete Symmetry Analysis of Vibrational Excitation in Benzene. *J. Chem. Phys.* **1993**, *99*, 827−835.